

BEDLOAD TRANSPORT OF SMALL RIVERS IN MALAYSIA

by

ZAHRA ZANGENEH SIRDARI

Thesis submitted in fulfilment of the requirements
for degree of
Doctor of Philosophy

May 2013

ACKNOWLEDGEMENTS

I would like to thank all the individuals and organizations who have helped or provided the guidance during the study. Among the organisations, firstly I would like to thank the Universiti Sains Malaysia who provided the opportunity to study in this university under fellowship scheme. I am also thankful to USM for all efforts from granting the study leave to providing all reports and drawings required for this thesis work.

First and foremost I would like to express my genuine gratitude to my supervisor, Prof. Dr. Hj Aminuddin Ab. Ghani for his supervision, advice and guidance. I really was honoured to have the opportunity to work under his supervision. Also I would like to special thanks to my second Supervisor Mr. Zorkeflee Abu Hasan for his guidance and technical support.

I would also like to thank River Engineering and Urban Drainage Research Centre (REDAC) and its staffs especially Mrs. Nor Mawati Mohamad, Mr. Mohd Sufian Osman, Mr. Rahim Ghazali and Mr. Khairul Nizam Abu for helping me in field measurements and data collection.

I don't have words to express my thanks to Dr. Farshid Bateni, in fact no words can express his generosity. All through this work he has provided his guidance and help in modelling and programming in MATLAB. I am also thankful to all officers, seniors, colleges and friends who helped one or another way to make possible this study.

Last but not least I would extend my word of thanks to my family specially my lovely sister Nasim who helped me during all this duration of my study.

TABLE OF CONTENTS

ACKNOWLEDGEMENTS.....	ii
TABLE OF CONTENTS.....	iii
LIST OF TABLES.....	vii
LIST OF FIGURES	x
LIST OF ABBREVIATIONS	xx
LIST OF SYMBOLS	xxi
ABSTRAK.....	xxiv
ABSTRACT	xxvi
CHAPTER 1 INTRODUCTION.....	1
1.1 Background.....	1
1.2 Problem Statement.....	3
1.3 Objective of the Investigation.....	5
1.4 Scope of Work.....	5
1.5 Structure of Thesis.....	6
CHAPTER 2 LITERATURE REVIEW	8
2.1 Introduction	8
2.2 Bedload Transport	8
2.3 Bedload Transport Analysis	9
2.4 Bed Load Transport Equations.....	12
2.4.1 Performance of Bedload Transport Equations	19
2.5 Regression Analysis	21
2.5.1 Linear Regression	21
2.5.2 Multiple Linear Regression.....	22
2.5.3 Least- Square Method	23
2.5.4 Polynomial Regression.....	24
2.5.5 Nonlinear Regression.....	24
2.6 Soft Computing Modelling.....	25

2.6.1	Genetic Programming (GP).....	26
2.6.2	Artificial Neural Network (ANN).....	28
2.7	Application of Soft Computing Modelling in Prediction of Bedload Transport	30
2.8	River Channel Confluence.....	36
2.9	Sediment Transport Modelling.....	41
2.9.1	SSIIM.....	48
2.9.1.1	SIMPLE Algorithm	49
2.9.1.2	Control Volume Scheme.....	49
2.9.1.3	SSIIM Application.....	50
2.10	Summary.....	55
CHAPTER 3 METHODOLOGY		58
3.1	Introduction	58
3.2	Study Area.....	59
3.3	River Hydrology and Hydraulic	61
3.3.1	Stream Flow Data.....	61
3.3.2	Water Level Record	61
3.3.3	Stage Discharge Data	62
3.3.4	Flood Frequency Analysis.....	63
3.4	Field Data Measurement.....	67
3.4.1	Flow Measurement.....	68
3.4.2	Geometry Data	70
3.4.3	Sediment Data	72
3.4.3.1	Bed Material	72
3.4.3.2	Bedload.....	73
3.5	Techniques for Bedload Prediction	75
3.5.1	Performance of Bedload Transport Equation.....	76
3.5.2	Dimensional Analysis	77
3.5.3	Nonlinear Regression Method (NLR).....	78
3.5.4	Artificial Neural Network (ANN).....	79
3.5.5	Genetic Programming Method (GP).....	80
CHAPTER 4 BEDLOAD TRANSPORT CHARACTERISTICS		82
4.1	Introduction	82
4.2	River Characteristics	83
4.2.1	Summary of River Data Collection.....	83
4.2.2	Typical Cross-Sections for the River Study Site.....	87

4.2.3	Parameter Affecting Bedload Transport	90
4.3	Particle Size Distribution.....	93
4.4	Evaluation of Bedload Size Distribution with Increasing Shear Stress.....	97
4.5	Fractional Transport Rate	102
4.6	Performance of Bedload Transport Equation	107
4.6.1	Assessment of Existing Equation for Kurau River	107
4.6.2	Prediction of Bedload Transport in Kurau River with Nonlinear Regression Method	109
4.6.3	Prediction of Bedload Transport in Kurau River by Genetic Programming	112
4.6.4	Combination of ANN and GP	117
4.6.5	Comparison of Bedload Equations for Kurau River	122
4.7	Development of Bedload Equation for Small Rivers (Kurau, Lui, Semenyih)	126
4.7.1	Assessment of Existing Equations for Small Rivers (Kurau, Lui and Semenyih)	127
4.7.2	Nonlinear Regression Result for Small Rivers (Kurau, Lui and Semenyih)	129
4.7.3	Artificial Neural Network Results	131
4.8	Sensitivity Analysis	134
4.9	Genetic Programming Result.....	136
4.9.1	Comparison of Bedload Equations for Small Streams.....	139
CHAPTER 5 RIVER CONFLUENCE SEDIMENT TRANSPORT MODELLING....		142
5.1	Introduction	142
5.2	SSIIM	143
5.3	SSIIM versions	144
5.4	Theoretical Basis	145
5.4.1	Water Flow Calculation	146
5.4.1.1	The k- ϵ turbulence model	146
5.4.1.2	Wall laws	147
5.4.2	Sediment Flow Calculation	148
5.5	Graphical Interface	149
5.6	Input Files.....	150
5.7	Output Files	151
5.8	Making a Grid in SSIIM.....	153
5.8.1	Grid Editor	156
5.8.2	Multiblock and One Block Grid.....	156

5.9	Sediment Flow Simulation in Confluence of Kurau and Ara River.....	160
5.9.1	Characteristics of Kurau -Ara Confluence.....	161
5.9.2	Input Data.....	163
5.9.3	Input Files	165
5.9.3.1	Control File.....	165
5.9.3.2	Timei File	166
5.9.4	Numerical Algorithms.....	169
5.9.5	Sensitivity Analysis.....	170
5.9.6	Calibration and Validation	171
5.9.6.1	Model Calibration.....	171
5.9.6.2	Model Validation	183
5.9.7	Short Term Changes in Bedload Transport, Bed Morphology and Bed Material Characteristics	186
5.9.7.1	Morphological Changes.....	188
5.9.7.2	Lateral bar.....	209
5.9.7.3	Bedload Transport Rates.....	211
5.9.7.4	Sediment Pattern.....	220
5.9.8	High Flow Modelling.....	229
CHAPTER 6 CONCLUSIONS AND RECOMMENDATIONS		236
6.1	Conclusion.....	236
6.1.1	Bedload Transport Characteristics	236
6.1.2	Estimating Bedload Transport.....	237
6.1.3	Sediment Transport in River Channel Confluence	238
6.2	Recommendations	240
REFERENCES		241
APPENDIX A		
APPENDIX B		
APPENDIX C		

LIST OF TABLES

TABLES	TITLE	PAGES
Table 2.1	Bedload transport equations, Deterministic Shear stress method	13
Table 2.2	Bedload transport equations, Deterministic Stream power method	14
Table 2.3	Bedload transport equations, Deterministic Energy slope method	14
Table 2.4	Bedload transport equations, Deterministic Regression method	15
Table 2.5	Bedload transport equations, Deterministic Discharge and velocity method	17
Table 2.6	Bedload transport equations, Deterministic Equal mobility method	17
Table 2.7	Bedload transport equations, Deterministic Probabilistic method	19
Table 2.8	Comparison of bedload equations and the ANN model (Sasal et al., 2009)	32
Table 2.9	Summary of the major foregoing studies considering the morphodynamics of channel confluences (Leite Ribeiro et al., 2012)	38
Table 2.10	Summary of Some 3D hydrodynamic/sediment transport Models (Papanicolaou et al, 2008)	44
Table 2.11	Applications for selected 3D models (Papanicolaou et al, 2008)	46
Table 3.1	Flood ranking for Kurau River at Pondok Tanjung	64
Table 3.2	Summary of flood frequency analysis for Kurau River at Pondok Tanjung	65
Table 3.3	Goodness of fit test with chi-squared statistic value	65
Table 3.4	Typical cross sections along Kurau River (19 June 2010)	70
Table 3.5	The common bedload transport equations	77
Table 3.6	Multigene GP range of initially defined parameters	81

Table 4.1	Range of field data	85
Table 4.2	Summary of large and medium rivers (Monalis and Wu, 2001)	86
Table 4.3	The classification of sediments by particle size according to the Wentworth scale	98
Table 4.4	Summary of bedload transport equations assessment	108
Table 4.5	Parameter estimates of experimental data based on equation (3-14)	110
Table 4.6	Statistical analysis of experimental data based on equation (3-14)	110
Table 4.7	Parameter estimates of experimental data base on equation (4-1)	111
Table 4.8	Statistical analysis of experimental data base on equation (4-1)	111
Table 4.9	Assessment of NLR equation	112
Table 4.10	Summary of results of ANN	119
Table 4.11	Comparison of bedload transport equations	124
Table 4.12	Summary of bedload transport equations assessment	127
Table 4.13	Parameter estimates of experimental data based on equation (4-7)	129
Table 4.14	Parameter estimates of experimental data based on equation (4-8)	130
Table 4.15	Statistical analysis of experimental data base on equation (4-7)	130
Table 4.16	Sensitivity analysis results for parameters	135
Table 4.17	Bedload equations assessment	140
Table 5.1	Comparison of Cont value for one and two block grid	159
Table 5.2	Sediment characteristics	165
Table 5.3	Comparison of Bedload transport rate	173

Table 5.4	Parameter calibrated in SSIIM	174
Table 5.5	Comparisons of water and bed level for $Q=15 \text{ m}^3/\text{s}$ (19 July 2012)	183
Table 5.6	Comparisons of water and bed level for $Q=43 \text{ m}^3/\text{s}$ (27 Sept 2012)	183
Table 5.7	Comparisons of water and bed level for $Q=11 \text{ m}^3/\text{s}$ (8 Oct 2012)	185
Table 5.8	Hydraulic condition during an event at Kurau_Ara confluence	187

LIST OF FIGURES

FIGURES	TITLE	PAGES
Figure 2.1	Schematic representation of sediment transport in a stream (Singh, 2005)	9
Figure 2.2	Comparison of the performance of the ANN with simple regression and analytical approximation equations (Caamano et al., 2006)	31
Figure 2.3	The ANFIS model for bed load sediment (Azamathulla et al., 2009)	33
Figure 2.4	Predicted bed load against measured bed load using ANFIS (Azamathulla et al., 2009)	33
Figure 2.5	Observed versus predicted sediment load by SVM for Langat, Kurau and Muda rivers (Azamathulla et al., 2010b)	34
Figure 2.6	Observed versus predicted sediment load by FFNN for Langat, Kurau and Muda rivers (Ab. Ghani et al., 2011)	35
Figure 2.7	Observed versus predicted sediment load by GEP for Langat, Kurau and Muda rivers (Ab. Ghani and Azamathulla, 2012; Azamathulla et al., 2010a; Chang et al., 2012; Zakaria et al., 2010)	35
Figure 2.8	(a) Measured bed levels after the flushing (b) Simulated bed levels after the flushing (Haun and Olsen, 2012)	52
Figure 2.9	Comparison of bed level changes: (a) measurements; (b) numerical simulation with uniform sediment; and (c) nonuniform sediment (Feurich and Olsen, 2011)	53
Figure 2.10	Comparison between measured values and simulation results at: (a) cross section 80; (b) cross section 60; and (c) cross section 20	53
Figure 2.11	Measured water depths before (a) and after (b) the flood, together with measured (c) and computed (d) bed elevation changes (Fischer-Antze et al., 2008).	54
Figure 3.1	Research framework for present study	58
Figure 3.2	Kurau River sub-basin and data collection sites	60

Figure 3.3	Ara -Kurau river	60
Figure 3.4	Pondok Tanjung stream flow station (5007421)	61
Figure 3.5	Discharge hydrograph for Kurau River at Pondok Tanjung	62
Figure 3.6	Water level chart for Kurau River at Pondok Tanjung	62
Figure 3.7	Stage-discharge relationship at Pondok Tanjung for 1996-2007	63
Figure 3.8	Flood frequency analysis using difference types of distribution	66
Figure 3.9	Langat River basin and data collection sites by Ariffin (2004)	67
Figure 3.10	Electromagnetic current meter	68
Figure 3.11	SonTek River Surveyor Hydroboard with optional GPS	69
Figure 3.12	River surveying at Ara River with river surveyor (ADP)	72
Figure 3.13	Van Veen grab for bed material sampling	73
Figure 3.14	Hand held Helley-Smith sampler for bed load sampling	75
Figure 3.15	Feed-forward multilayer network	80
Figure 4.1	Cross section KRU1 along Kurau River	87
Figure 4.2	Cross section KRU2 along Kurau River	87
Figure 4.3	Cross section KRU3 along Kurau River	88
Figure 4.4	Cross section KRU4 along Kurau River	88
Figure 4.5	Cross section KRU5 along Kurau River	89
Figure 4.6	Cross section A1 along Ara River	89
Figure 4.7	Scatter plot of bedload transport rate against discharge	90
Figure 4.8	Scatter plot of bedload transport rate against velocity	90
Figure 4.9	Scatter plot of bedload transport rate against width	91

Figure 4.10	Scatter plot of bedload transport rate against water depth	91
Figure 4.11	Scatter plot of bedload transport rate against B/Y ratio	91
Figure 4.12	Scatter plot of bedload transport rate against hydraulic radius	92
Figure 4.13	Scatter plot of bedload transport rate against area	92
Figure 4.14	Scatter plot of bedload transport rate against slope	92
Figure 4.15	Scatter plot of bedload transport rate	93
Figure 4.16	Bedload frequency distribution size of upstream (KRU5) and downstream (KRU1) of Kurau River	95
Figure 4.17	Particle size distributions of bedload and bed material samples for Kurau River.	96
Figure 4.18	Comparison of particle size distributions of bedload samples for upstream and downstream of Kurau River in same discharge.	97
Figure 4.19	Mean bed load grain size distributions for shear stress bands arranged in order of increasing shear stress (upstream of Kurau River KRU5).	98
Figure 4.20	Mean bed load grain size distributions for shear stress bands arranged in order of increasing shear stress (downstream of Kurau River KRU1).	100
Figure 4.21	Variation in grain size at the 10th, 16th, 30th, 50th, 84th and 90th percentiles of the bedload size distribution with increasing shear stress.	101
Figure 4.22	Transport ratio as a function of grain size at upstream (a) the transport ratio P_i/f_i where p_i is the proportion of each size fraction i present in transported material and f_i is the proportion of each size fraction in the bed material (b) the scaled fractional transport rate computed as $q_b p_i/f_i$, where q_b is the sediment transport rate.	103
Figure 4.23	Transport ratio as a function of grain size at downstream (a) the transport ratio P_i/f_i (b) the scaled fractional transport rate $q_b p_i/f_i$.	104
Figure 4.24	Comparison of predicted and measured bedload rates for Kurau River	108

Figure 4.25	Bedload rating curve along Kurau River	109
Figure 4.26	Validation of NLR equation in Kurau River	112
Figure 4.27	Expression genes for GP formulation	114
Figure 4.28	Measured versus predicted values of T_b for the training data set.	115
Figure 4.29	Measured versus predicted values of T_b for testing data set.	116
Figure 4.30	Measured versus predicted values of T_b for validation data set.	116
Figure 4.31	Measured versus predicted values of T_b for all data set.	117
Figure 4.32	Measured versus predicted values of T_b by GP-ANN	118
Figure 4.33	Measured versus predicted values of T_b by ANN for training data set	119
Figure 4.34	Measured versus predicted values of T_b by ANN for testing data set	120
Figure 4.35	Measured versus predicted values of T_b by ANN for validation data set	121
Figure 4.36	Measured versus predicted values of T_b by ANN for total data set	121
Figure 4.37	Measured versus predicted values of T_b by ANN-GP	122
Figure 4.38	Comparison of bedload rating curve for Kurau River	125
Figure 4.39	Comparisons of predicted and measured bedload rates for Kurau River	125
Figure 4.40	Bedload rating curve for three rivers	126
Figure 4.41	Performance of existing bedload transport formula in Kurau, Lui and Semenyih rivers.	128
Figure 4.42	Measured versus predicted values of T_b for total data set modelled by NLR	131
Figure 4.43	Measured versus predicted values of T_b by ANN for the training data set	133
Figure 4.44	Measured versus predicted values of T_b by ANN for testing data	133

	set	
Figure 4.45	Measured versus predicted values of T_b by ANN for validation data set	134
Figure 4.46	Measured versus predicted values of T_b by ANN with for total data set.	134
Figure 4.47	Measured versus predicted values of T_b for the training data set.	137
Figure 4.48	Measured versus predicted values of T_b for testing data set	138
Figure 4.49	Measured versus predicted values of T_b for total dataset	138
Figure 4.50	Measured versus predicted values of T_b for validation dataset	139
Figure 4.51	Comparison of bedload rating curve for small streams	141
Figure 4.52	Comparisons of predicted and measured bedload rates for small streams by different models	141
Figure 5.1	Structured grid	144
Figure 5.2	Unstructured grid	145
Figure 5.3	SSIIM graphical interface	150
Figure 5.4	SSIIM flowchart (Olsen, 2011)	153
Figure 5.5	Koordina file	154
Figure 5.6	3D grid generation	155
Figure 5.7	Koosurf file	155
Figure 5.8	Two block grid	157
Figure 5.9	One block grid	158
Figure 5.10	View of the confluence of the Kurau and Ara rivers	162
Figure 5.11	Contour bed level of the Kurau-Ara confluence	162
Figure 5.12	Sediment distribution size of bedload in Kurau River branch	163

Figure 5.13	Sediment distribution size of bedload in Ara River	164
Figure 5.14	Sediment distribution size of bedload in main Kurau River	164
Figure 5.15	Control file used in SSIIM modelling	167
Figure 5.16	Time File	168
Figure 5.17	Comparison of Bedload transport rate	172
Figure 5.18	Measured and simulated average velocity in Ara mouth	175
Figure 5.19	Measured and simulated average velocity in Kurau mouth	175
Figure 5.20	Comparison cross-sectional bed level and average velocity a) simulated b) Measured, April 2012 at Ara River	176
Figure 5.21	Comparison cross-sectional bed level and average velocity a) simulated b) Measured, April 2012 at Kurau River	177
Figure 5.22	Measured bed level (April 2012)	178
Figure 5.23	Simulated contour bed level	178
Figure 5.24	Comparison cross sectional bed level in different condition of Ara and Kurau confluence (Measured BL, April 2012)	179
Figure 5.25	Comparison of measured and simulated Longitudinal bed level at downstream of confluence (AA') (Measured BL, April 2012)	180
Figure 5.26	Scatter plot of measured bed level against simulated bed level (April 2012)	180
Figure 5.27	Comparison of measured and simulated water level at downstream of confluence (AA') (April 2012)	181
Figure 5.28	Scatter plot of measured water level against simulated water level (April 2012)	181
Figure 5.29	Measured water level (April 2012)	182
Figure 5.30	Simulated water level	182
Figure 5.31	Comparisons of water and bed level (AA') for $Q=15 \text{ m}^3/\text{s}$ (19 July 2012)	184

Figure 5.32	Comparisons of water and bed level (AA') for Q=15 m ³ /s (20 July 2012)	184
Figure 5.33	Comparisons of water and bed level (AA') for Q=11 m ³ /s (8 Oct 2012)	185
Figure 5.34	Morphology of Kuaru -Ara confluence	187
Figure 5.35	Longitudinal bed change profile of Ara and downstream of confluence after Q=15m ³ /s	189
Figure 5.36	Longitudinal bed change profile of Kurau and downstream of confluence after Q=15m ³ /s	189
Figure 5.37	Bed morphology after Q=15 m ³ /s	190
Figure 5.38	Change in bed morphology after Q=15m ³ /s. Zone of erosion and deposition during each period are illustrated with colour change from white as deposition to black as erosion.	190
Figure 5.39	Channel cross section profiles, Q=15m ³ /s (Measured bed level April 2012)	191
Figure 5.40	Bed morphology after Q=31 m ³ /s	192
Figure 5.41	Channel cross section profiles, Q=31m ³ /s	193
Figure 5.42	Longitudinal bed change profile of Ara and downstream of confluence between Q=15m ³ /s and Q=31m ³ /s (Measured bed level April 2012)	194
Figure 5.43	Longitudinal bed change profile of Kurau and downstream of confluence between Q=15m ³ /s and Q=31m ³ /s (Measured bed level April 2012)	194
Figure 5.44	Change in bed morphology between Q=15m ³ /s and Q=31m ³ /s. Zone of erosion and deposition during each period are illustrated with colour change from white as deposition to black as erosion.	195
Figure 5.45	Flow separation Mr>1	196
Figure 5.46	Flow separation at Ara- Kurau confluence (Mr>1)	196
Figure 5.47	Bed morphology after Q=43m ³ /s	197
Figure 5.48	Channel cross section profiles, Q=43m ³ /s	199

Figure 5.49	Longitudinal bed change profile of Ara and downstream of confluence between $Q=31\text{m}^3/\text{s}$ and $Q=43\text{m}^3/\text{s}$ (Measured bed level April 2012)	200
Figure 5.50	Longitudinal bed change profile of Kurau and downstream of confluence between $Q=31\text{m}^3/\text{s}$ and $Q=43\text{m}^3/\text{s}$ (Measured bed level April 2012)	200
Figure 5.51	Change in bed morphology between $Q=31\text{m}^3/\text{s}$ and $Q=43\text{m}^3/\text{s}$. Zone of erosion and deposition during each period are illustrated with colour change from white as deposition to black as erosion.	201
Figure 5.52	Longitudinal bed change profile of Ara and downstream of confluence between $Q=43\text{m}^3/\text{s}$ and $Q=35\text{m}^3/\text{s}$ (Measured bed level April 2012)	202
Figure 5.53	Longitudinal bed change profile of Kurau and downstream of confluence between $Q=43\text{m}^3/\text{s}$ and $Q=35\text{m}^3/\text{s}$ (Measured bed level April 2012)	202
Figure 5.54	Bed morphology after $Q=35\text{m}^3/\text{s}$	203
Figure 5.55	Change in bed morphology between $Q=43\text{m}^3/\text{s}$ and $Q=35\text{m}^3/\text{s}$. Zone of erosion and deposition during each period are illustrated with colour change from white as deposition to black as erosion.	203
Figure 5.56	Channel cross section profiles, $Q=35\text{m}^3/\text{s}$	204
Figure 5.57	Bed morphology after $Q=13\text{m}^3/\text{s}$	205
Figure 5.58	Flow separation $Mr < 1$	206
Figure 5.59	Longitudinal bed change profile of Ara and downstream of confluence between $Q=35\text{m}^3/\text{s}$ and $Q=13\text{m}^3/\text{s}$ (Measured bed level April 2012)	206
Figure 5.60	Longitudinal bed change profile of Kurau and downstream of confluence between $Q=35\text{m}^3/\text{s}$ and $Q=13\text{m}^3/\text{s}$ (Measured bed level April 2012)	207
Figure 5.61	Change in bed morphology between $Q=35\text{m}^3/\text{s}$ and $Q=13\text{m}^3/\text{s}$. Zone of erosion and deposition during each period are illustrated with colour change from white as deposition to black as erosion.	207
Figure 5.62	Channel cross section profiles, $Q=13\text{m}^3/\text{s}$	208
Figure 5.63	longitudinal profile of lateral change in different flow momentum	210

Figure 5.64	Cross sectional lateral change in different flow momentum	210
Figure 5.65	Bed load transport rating curve in Ara and Kurau River branch	211
Figure 5.66	Bed load transport rate value by SSIIM against the calculated bedload transport rate with Eq. 4.11	212
Figure 5.67	Bed morphology and spatial distribution of bedload transport rate $Mr=0.9$.	213
Figure 5.68	Bed morphology and spatial distribution of bedload transport rate $Mr=1.3$.	214
Figure 5.69	: Bed morphology and spatial distribution of bedload transport rate $Mr=2.6$.	215
Figure 5.70	Bed morphology and spatial distribution of bedload transport rate $Mr=0.7$.	216
Figure 5.71	Shear layer and distinct vortices about vertical axes at RSK1	218
Figure 5.72	Shear layer in the confluence of Ara and Kurau	218
Figure 5.73	Bedload rate in cross sections at downstream of confluence	219
Figure 5.74	Distribution of bed median size, $D_{50} Q=15 \text{ m}^3/\text{s}$, $Mr<1$	222
Figure 5.75	Bed shear stress in confluence $Q=15\text{m}^3/\text{s}$	223
Figure 5.76	Distribution of bed median size at high flow, $D_{50} Q=43 \text{ m}^3/\text{s}$, $Mr>1$	224
Figure 5.77	Bed shear stress in confluence $Q=43\text{m}^3/\text{s}$	225
Figure 5.78	Distribution of bed median size at low flow, $D_{50} Q=13 \text{ m}^3/\text{s}$, $Mr<1$	226
Figure 5.79	Bed shear stress at low flow $Q=13\text{m}^3/\text{s}$	228
Figure 5.80	Hydrograph of the October 2007 flood	229
Figure 5.81	The morphology of Kurau-Ara confluence before flood	230
Figure 5.82	Bed morphology of Kurau-Ara confluence after flood	231

Figure 5.83	Change in bed morphology after $Q=191.32\text{m}^3/\text{s}$. Zone of erosion and deposition during each period are illustrated with colour change from white as deposition to black as erosion.	232
Figure 5.84	Longitudinal bed change profile of downstream of confluence	232
Figure 5.85	Modelled cross section changes before and after flood 2007	234
Figure 5.86	Bed morphology and spatial distribution of bedload transport rate ($Q=191.32\text{m}^3/\text{s}$)	235

LIST OF ABBREVIATIONS

Abbreviation	Description
ANN	Artificial Neural Network
ADP	Acoustic Doppler Profiler
ASCE	American Society of Civil Engineers
ARI	Average Recurrence Interval
BL	Bed Level
CFD	Computational Fluid Dynamics
CHZ	Confluence Hydrodynamic Zone
DID	Department of Irrigation and Drainage
DR	Discrepancy Ratio
EDM	Electronic Distance Meter
GA	Genetic Algorithm
GP	Genetic Programming
GPS	Global Positioning System
MAE	Mean Absolute Error
Mr	Momentum ratio
NLR	Non Linear Regression
RMSE	Root Mean Square Error
SSIIM	Sediment Simulation In Intakes with Multiblock option
SVM	Support Vector Machines
WL	Water Level
WS	Water Surface

LIST OF SYMBOLS

Symbol	Description
A	Flow area (m^2)
b	Section width of the channel (m)
B	River channel width (m)
$Cs = (B/y_0)$	Conveyance shape
Cz	Chezy resistance coefficient
$d_l = \theta - \theta_{cr}$	The Shield's parameter difference
$d_3 = d_s v_{av}$	The average flow velocity with sediment particle diameter (m^2/s^2)
d_{50}, d, D_{50}	Sediment diameter where 50% of bed material is finer
d_i	Size of particle intermediate axis for which $i\%$ of sample of bed material is finer
d_{50sub}	Submerged median particle size
d_s	Sediment particle diameter
Dgr	Dimensionless particle parameter
E	East
f	Friction factor
f_s	Wilcock's friction coefficient
f_i	Proportion of each size fraction present in bed material
Fr	Froude number
g	Acceleration due to gravity
g_b	Sectional bed load transport rate
Gs	Sediment specific gravity = 2.65
G_r	Gradation coefficient

h_s	Width of Helley-Smith sampler nozzle
n	Manning's roughness coefficient
N	North
P	Wetted perimeter of cross section of flow (m)
Q	Flow discharge (m^3/s)
Q_s	Bed material discharge for all size fractions (m^3/s)
q	Water discharge per unit width
q_b	Bedload discharge per unit width
$q_b p_i / f_i$	Scale fractional transport rate
P_i	Proportion of each size fraction present in transported material
R	Hydraulic Radius
R^2	Coefficient of determination
Re	Reynolds number
R/d_{50}	Standardization with hydraulic radius
S_f	Channel slope
S_0	Water surface slope
T_b	Bed load transport rate (kg/s)
T_j	Total bed load transport rate (kg/s)
T_s	Suspended load transport rate (kg/s)
T_t	Suspended load discharge (m^3/s)
T	Time the bed load sampler on the bed
u^* and u^*_{cr}	Shear and critical shear velocity
U	Inequality coefficient
V	Average flow velocity

\overline{w}_t	Mean weighted bed load sample of vertical for n section
w	weights on the network connections
y_0, y	Flow depth
y/B	width scale ratio
Z	Vertical coordinate (elevation)
α_s	Wiberg and Smith's coefficient
β	Standardized coefficient
γ and γ_s	Specific weight of water and sediment
Γ	Diffusion coefficient
θ and θ_{cr}	Shields' and critical Shields' parameters for initiation of motion
κ	von Karman constant =0.4
μ	Dynamic viscosity of water
Π	Shear stress due to relative density
ρ and ρ_s	Density of water and sediment
τ and τ_{cr}	Shear and critical shear stress at the bed
ν	kinematic viscosity
Φ_b	Dimensionless intensity of the bedload rate
ω_s	Fall velocity of sediment particles (d_{50})
ω_{s*}	Standardized fall velocity due to sediment particle

PENGANGKUTAN BEBAN ENDAPAN DASAR UNTUK SUNGAI KECIL DI MALAYSIA

ABSTRAK

Pengangkutan beban endapan dasar merupakan komponen penting proses dinamik sungai dan penganggaran kadar pengangkutan beban endapan dasar adalah penting untuk pengiraan variasi morfologi sungai untuk tujuan keselamatan umum, pengurusan sumber air dan alam sekitar yang mampan. Pelbagai persamaan beban endapan yang terkenal adalah terhad kepada kajian eksperimen saluran dalam makmal atau kajian tapak. Persamaan ini yang dipengaruhi oleh kebolehpercayaan dan perwakilan data yang digunakan dalam menentukan pembolehubah dan pemalar memerlukan parameter yang kompleks dalam penganggaran pengangkutan beban endapan. Oleh itu, satu persamaan baru yang mudah dan tepat adalah perlu untuk kegunaan di sungai-sungai kecil. Dalam kajian ini, data yang mudah diperolehi seperti kadar alir, kedalaman sungai, kecerunan sungai dan saiz diameter zarah endapan permukaan d_{50} daripada tiga sungai kecil di Malaysia digunakan untuk meramal pengangkutan endapan dasar. Model genetic programming (GP) dan artificial neural network (ANN) adalah berguna dalam menafsir data tanpa sebarang had untuk pangkalan data yang luas digunakan sebagai alat untuk pemodelan pengangkutan beban endapan untuk sungai-sungai kecil. Keupayaan GP dan ANN untuk meramal data hujan adalah memuaskan. Model yang diperolehi menunjukkan kejituan yang tinggi dengan ketepatan keseluruhan sebanyak 97% untuk ANN dan 93% untuk GP berbanding dengan kaedah konvensional dan persamaan empirical.

Satu model numerikal tiga dimensi telah digunakan untuk mengkaji morfologi dasar dan pengangkutan beban endapan dasar sungai di pertemuan Sungai Ara dan

Kurau untuk jangka masa pendek dengan kadar alir tinggi pada 100 ARI. Model tiga dimensi SSIIM2 dengan k-epsilon aliran gelora yang merupakan model pengiraan bendalir dinamik dengan grid adaptif, bukan ortogon dan tidak berstruktur telah digunakan untuk pemodelan hidrodinamik pertemuan sungai. Model numerikal ini telah diuji dengan data dari kajian tapak di pertemuan Ara-Kurau. Ketepatan yang memuaskan telah didapati di antara data endapan dasar dan aras dasar yang dianggar dengan yang dicerap di tapak. Kajian menunjukkan bahawa model numerikal merupakan alat yang berguna dalam meramal kadar pengangkutan beban dasar di kawasan yang bersekitaran dinamik kompleks. Keputusan menunjukkan bahawa perubahan hidrologi jangka pendek boleh mempengaruhi morfo-dinamik pertemuan Ara-Kurau. Untuk keadaan aliran yang berbeza, pengangkutan endapan dasar berhampiran pinggir lapisan ricih dan juga lapisan ricih yang menyebabkan aliran gelora menunjukkan peningkatan aliran gelora menyumbang kepada peningkatan kapasiti pengangkutan endapan beban dasar sungai. Keputusan simulasi menunjukkan taburan saiz zarah beting pasir di tepi hilir pertemuan sungai adalah tidak berubah dimana saiz median tidak berubah sepanjang tempoh kajian manakala saiz zarah di hulu beting pasir adalah lebih dipengaruhi oleh keadaan aliran.

BEDLOAD TRANSPORT OF SMALL RIVERS IN MALAYSIA

ABSTRACT

Bedload transport is an essential component of river dynamics and estimation of bedload transport rate is important for practical computations of river morphological variations because the transport of sediment through river channels has major effects on public safety, water resources management and environmental sustainability. Numerous well-known bedload equations are derived from limited flume experiments or field conditions. These time-consuming equations, based on the relationship between the reliability and representativeness of the data utilized in defining variables and constants, require complex parameters to estimate bedload transport. Thus, a new simple equation based on a balance between simplicity and accuracy is necessary for using in small rivers. In this study the easily accessible data including flow discharge, water depth, slope, and surface grain diameter d_{50} from the three small rivers in Malaysia used to predict bedload transport. Genetic programming (GP) and artificial neural network (ANN) models that are particularly useful in data interpretation without any restriction to an extensive database are presented as complementary tools for modelling bed load transport in small streams. The ability of GP and ANN as precipitation predictive tools showed to be acceptable. The developed models demonstrate higher performance with an overall accuracy of 97% for ANN and 93% for GP compared with other traditional methods and empirical equations.

A three-dimensional numerical model was applied to study the bed morphology and bedload transport of the junction of Ara and Kurau rivers for short term event and for high flow with 100 ARI. SSIIM2 a 3D, k-epsilon turbulence

computational fluid dynamics model with an adaptive, non-orthogonal and unstructured grid has been used for modelling the hydrodynamic of confluence. The numerical model was tested against field data from Ara-Kurau confluence. Satisfactory agreement was found between computed and measured bedload and bed elevation in the field. The study indicates that numerical models became a useful tool for predicting the bedload transport rate in such complex dynamic environment. The results have demonstrated that the short term hydrologic variability can considerably influence the morphodynamics of Ara-Kurau channel confluence and for the different flow conditions the bedload transported near to edge of shear layer. The coincidence of the shear layer that was generated the considerable turbulence indicated that the increasing turbulence levels contribute substantially to the required increase in bedload transport capacity. The simulation results showed the grain size distribution on the bar at the downstream junction corner is remarkably constant and the particle size in the upstream part of the bar is more affected by the changes in flow conditions than the downstream end where the median diameters not varied during the period.

CHAPTER 1

INTRODUCTION

1.1 Background

Bedload transport is an essential component of river dynamics that depends on water flow, river morphology and response of sediment particles to applied stress and their mutual interactions. Estimation of bedload transport rate is important for practical computations of river morphological variations because the transport of sediment through river channels has major effects on public safety, water resources management and environmental sustainability (Yeganeh-Bakhtiary et al. 2009; Frey and Church 2011).

The relationship between bedload transport rates and hydraulic variables is extremely complex because of various characteristics of alluvial rivers such as sediment transport, the interaction between sediment supply and bed surface adjustment, and the hydrodynamics of bedform progress. The difficulties associated with bedload field measurement causes a long history of interest in developing equations for the prediction of bedload transport. Numerous well-known bed load equations were derived from limited flume experiments or field conditions (Bagnold, 1980; Camenen and Larson, 2005; Yang, 1996). Although morphologist and engineers have gained profound insight into the mechanics of bedload transport ever since the development of the duBoys equation (du Boys, 1879) (the first physically based bedload transport equation) a simple question still cannot be answered: for given sedimentary and hydraulic characteristics, what is the rate of bedload transport in an alluvial channel? In other words, there is no single bedload equation that can be applied universally to all rivers and no completely objectively or universally

applicable guidelines exist to facilitate the selection of an appropriate formula as the bedload transport function (Almedeij and Diplas, 2003; Gomez and Church, 1989; Simons and Şentürk, 1992; Yang and Huang, 2001). To overcome the difficulties of developing the equations based on a balance between simplicity and accuracy, new mathematical modelling methods can be used to improve the sensitivity and performance of the prediction equations; the simple formula can be adopted to estimate the bedload transport of small streams.

River flow, sediment transport and morphological processes are among the most complex and least understood processes or phenomena in nature. A river confluence has always been a challenging subject for river hydrodynamics and morphodynamics considerations due to complex flow phenomena and processes occurring in both the confluence and the downstream of confluence channel. The complexity of the phenomena and processes arises from the strong three dimensional flow effects resulting from several principal factors, including a) the discharge or momentum ratio between tributary and main stream b) the planform shape of upstream and post confluence channel and angle of the confluence c) the difference between the levels of tributary and main stream (Best, 1986; Leite Ribeiro et al., 2012; Rhoads, 1996).

In the last decade, the development of hydrodynamic existing methods and new methods and tools for investigation of complex flows especially in three dimensions has greatly improved the understanding of the dynamics of confluences (Biron et al., 2004; Bradbrook et al., 2000; Weerakoon and Tamai, 1989) Therefore, laboratory studies combined with field observations are needed to link a global quantitative

model of channel confluences for better understanding of complex hydrodynamic and morphodynamics of river channel confluences .

1.2 Problem Statement

River sedimentation problems are assuming increasing importance in many Malaysian rivers and can represent a key impediment to sustainable development. Despite more than six decades of research, sedimentation is still probably the most serious technical problem faces by water resource manager and engineers. Such problems include accelerated soil erosion, reservoir sedimentation and the wider impact of sediment on aquatic ecology, river morphology and water resource exploitation.

Sediment transport in small streams is diverse and highly variable due to the various characteristics of channel morphology. Numerous well-known bed load equations were derived from limited flume experiments or field conditions (Bagnold, 1980; Camenen and Larson, 2005; Yang, 1996). In such conditions, equations based on the relationship between the reliability and representativeness of the data utilized in defining reference values, constants, and relevant coefficients are time consuming and required complex parameter to estimate bed load transport. Although a known equation may produce reasonable predictions of bedload transport rates in a particular stream reach at a particular time, the same equation usually overpredict or underpredict the observed bed load transport by a different order of magnitude when applied to a different river or even to the same river at a different time. Therefore, there is a real need to consider and derive a simple equation to predict bedload transport with easy accessible data for specific conditions.

Kurau River is selected as the case study due to its importance as a main domestic water supply and Kerian irrigation scheme areas in the state of Perak. Bukit Merah reservoir and the dam that was constructed approximately at the mid section of the Kurau River system requires the river management such as controlling the sediment transport and consideration changes in river morphology.

Human activity includes the recently railway construction, changes in land use from 2004 to 2015 according to the Taiping Town Council on Larut Matang Local Plan 2015 (Hamidun, 2010), and increasing river sand mining makes change to river hydrology and increase in sediment load along the river. The loss of river capacity due to sedimentation can have a serious impact on water resources development by reducing the supply of irrigation water, water supply, and the effectiveness of flood control schemes. Kurau River sedimentation becomes the main cause of frequent flooding in urban areas(Hamidun, 2010). The blockage of hydraulic structure of higher sediment yield and overflowing water cause serious damages to the environment, infrastructures and also has an effect on the social activity. Therefore, integrated sediment management in Kurau River is one of the highest concerns of governments and engineers.

Upstream of Kurau River as a selected case study consisting of two main river tributaries namely Kurau River and Ara River. The river condition and morphology can be different in each section of river. One of the complex and effective place of the river due to sediment transport behaviour is the confluence of two river channels. The sediment transport in the confluences changes periodically in different flow

condition. Evaluation of the bedload transport in confluence requires the use of numerical modelling techniques as the simple empirical equation individually cannot evaluate such complex condition.

1.3 Objective of the Investigation

- To establish bedload particle sizes characteristic and its effect on bedload transport
- To estimate the bedload transport rate in small streams by statistical analysis, artificial neural network and genetic programming and evaluate the prediction methods.
- To evaluate the changes in bed load sediment transport, bed morphology and spatial pattern of bed material in response to flow discharge variability in river channel confluence with a 3D numerical model.

1.4 Scope of Work

This study was carried out on Kurau River, a natural stream in Perak, Malaysia. Herein, the genetic programming, artificial neural network and nonlinear regression models which are particularly useful in modelling processes with data interpretation without any restriction to an extensive database, are employed as a complimentary tool for modelling bed load transport in small streams.

Hydraulic and sediment data were taken at six locations along Kurau River and combine with the Lui and Semenyih Rivers data (Ariffin, 2004) for development of bedload transport equation.

The performance of the genetic programming, artificial neural network and statistical (nonlinear regression) models were evaluated and compared with six bedload transport equations such as Meyer-Peter and Müller (1948), based on energy slope method and Rottner (Yang, 1996), Chang (Cheng, 2002), Julien (2002) and vanRijn (1993) based on regression method and Wong and Parker (2006) based on the shear stress method.

SSIIM, a three dimensional computational fluid dynamic program was used in this study for modelling the Ara-Kurau confluence. It solves the Navier-Stokes equations in a three-dimensional non-orthogonal grid for flow and the convection-diffusion equation for sediments. SSIIM uses the "k-epsilon" model for turbulence, the control volume method with the SIMPLE algorithm.

The field site for the modelling is the junction of the Kurau and Ara rivers in Pondok Tanjung at the upstream of the Bukit Merah reservoir in Perak. The study was carried at confluence limited in areas with approximately 141.5 m in length and 111.5 m in width.

1.5 Structure of Thesis

The thesis consists of six chapters, organised as follows:

Chapter 1 gives a brief introduction on the bedload transport and objective of study, scope of work and sedimentation problem.

Chapter 2 has a brief review about the headworks and different types of traditional and innovative methods to estimate bedload transport rate. Selection of

the models and summary of model application relevant to this study was briefed in this section.

Chapter 3 states some facts about the study for which this study has been done. Data collection, data analysis and some soft computing method for predicting bedload transport were also explained in this chapter.

Chapter 4 describes bedload characteristics and results of prediction method of bedload transport.

Chapter 5 illustrates the theory behind the SSIIM. It is not possible to go into further detail due to dearth of space and time. Maximum reference has been made to user manual for SSIIM. Manual in itself is quite explanatory. It is readily available over the net. One of the nicety of this program or the liberality of the developer is that this program is freely available over net with manual. This chapter also provides the information the way the program is used herby. It includes the bedload transport characteristic in confluence zone, which is the main theme of this work.

Chapter 6 summarized the conclusions of study and recommendations for future study. Bibliography and appendices are enclosed at the end of this thesis.

CHAPTER 2

LITERATURE REVIEW

2.1 Introduction

Bedload transport is an important physical process in defining the morphological development of alluvial rivers (Barry et al., 2008). Bedload transport rate estimation is needed for the realistic computations of river morphological variations because the transport of sediment through river channels has a major disbursement for public safety, water resources management, and environmental sustainability (Frey and Church, 2011; Yeganeh-Bakhtiary et al., 2009).

Sediment transport in small streams is greatly variable and different due to the various characteristics of channel morphology. The hydraulic geometry of channels in small streams is affected by various parameters. Each channel section is in many ways unique because it is influenced by its own particular history of flow conditions, sediment transport, and distribution of channel roughness elements, and management activities, all of which should be considered in bedload transport estimation (Beschta and Platts, 1986).

2.2 Bedload Transport

Streams typically carry large amount of sediment to lower elevation. This material is called the stream load, and it is divided into bedload, suspended load, and dissolved load (Figure 2.1). Bedload transport refers to the movement of bed sediments along the stream bed by rolling, sliding, or jumping (Wang et al., 2011), and is absolutely dependent on the river's morphological characteristics.

Bedload transport as a fundamental physical process in alluvial rivers provides the major process relation between the hydraulic and sediment conditions that manage river channel morphology. To clarify the causes and effect of changes in channel morphology and also to make informed management decisions that affect a river's function, it will require a good knowledge regarding the role of bedload movement in forming and maintaining channel geometry (Gomez, 2006; Goodwin, 2004).

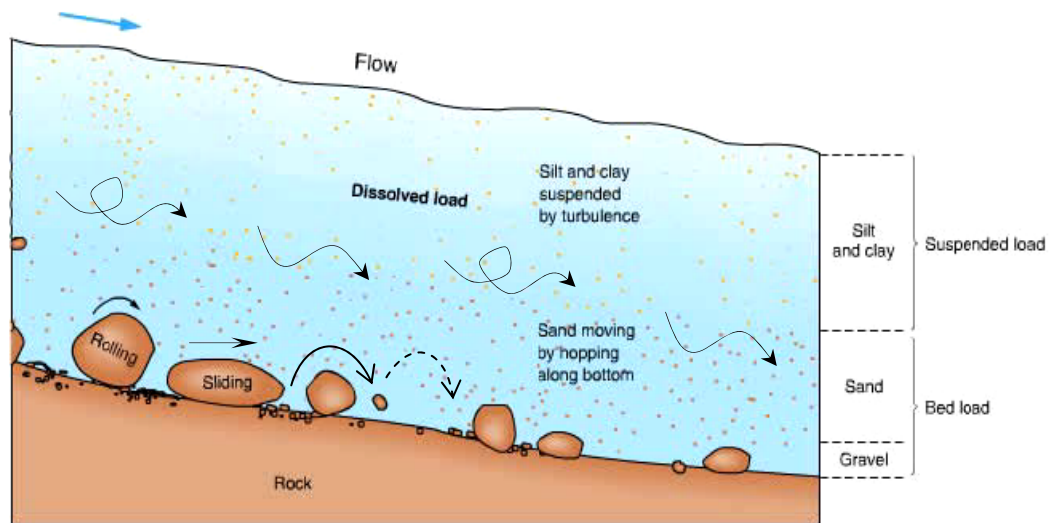


Figure 2.1: Schematic representation of sediment transport in a stream (Singh, 2005)

2.3 Bedload Transport Analysis

Over the years sediment transport such as sand or gravel under hydraulic conditions is objective by geologists and engineers to understand the grain-size distributions found in sedimentary deposits and to study the size sorting process (Niekerk et al., 1992).

Sediment size moves as bedload in rivers is important in sediment load calculations and stability analyses. Moreover, knowledge of sediment sorting patterns and processes is important because it is essential in understanding modern and older fluvial systems, boundary roughness and heavy mineral advancement (Carling and Dawson, 1996; Force et al., 1991; Robert, 1990) .

Bedload size distribution and bed material particle size specifications are required to determine the sediment transport process (Ghoshal et al., 2010). The extracted parameter from affective factors on sediment transport can be used as a basis for the prediction of sediment transport rates. Bedload size and bed material demonstrate the size of material transported downstream and the size of material accumulating upstream. The characteristics of bed material are indicators of the resistance of the armoring layer and the ability of the stream to move surface particles (Wilcock and Kenworthy, 2002).

Bedload transport in rivers is basically the process of movement of individual particles. The individual sediment size and the characteristic of the bed sediment influence sediment transport. However, the arrangement of different grain sizes (Buffington and Montgomery, 1997; Church, 2006) and patterns, such as sheltering, imbrications, armoring, and variations in sorting, can also affect the stabilities and in turn the critical shear stress required to carry the sediment (Charlton, 2007; Clayton, 2010).

The characteristics of particle movement courses are essential to sediment transport theory, the development of channel morphology, and are the basis for a

method of measuring the bed load transport rate (Pyrce and Ashmore, 2003). Measurement on the variations in transport rates between particles of different sizes is required when riverbed have different particle sizes, particularly in gravel bed rivers due to the wide range of particle size. The movement of individual particles depend on their relative as well as absolute size was shown by many researches that using the field and laboratory sediment transport data. The overall transport rate of mixed-sized sediments and the effects of changing sands and gravel contents were studied in a laboratory flume (Curran and Wilcock, 2005; Wilcock and Crowe, 2003; Wilcock et al., 2001). In an attempt to assess the evolution of bedload grain size, Kuhnle (1989) worked on a stream with sand and gravel mixture. He discovered that sediment size had a bimodal distribution and that sand fraction was entrained at lower velocities rather than gravel fraction.

Fractional bedload transport has been studied in the field (Bond, 2004; Diplas, 1992; Kuhnle, 1989; Kuhnle, 1992; Powell et al., 2001; Wathen et al., 1995) and in the laboratory (Wilcock and McArdeell, 1993; Wilcock and Southard, 1989). A supplementary study was performed on sand, gravel, and sand–gravel mixture to determine the critical shear stress of each size fraction from five different sediment beds (Kuhnle, 1993). All grain sizes of sand and gravel beds start to move at a nearly identical shear stress. However, a constant relationship between critical shear stress and grain sizes was observed in sand size sediments for the beds composed of sand–gravel mixture, but for the gravel fraction, the critical shear stress increased with the increase in size. Further studies show that most sand sizes may have nearly equal entrainment mobility in both laboratory and field studies (Church et al., 1991; Parker et al., 1982; Wilcock and Southard, 1989). The experiments were conducted in a

flume with mixed-sized sediments (Lanzoni and Tubino, 1999). Results show that the capacity of the sediment transport be modified by the different mobility of the diverse grain-size fractions in the mixture and induce a longitudinal and transverse pattern in sorting.

Powell et al. (2001) classified a second major threshold of approximately $4.5\tau_c$ in the Nahal Eshtemo River. Below this threshold, size selective occurs and above it, a condition approaching equal mobility occurs. This range of threshold is about twice as that as in sediment mixtures with comparable sorting coefficients in flume studies (Wilcock and McArdell, 1993).

2.4 Bed Load Transport Equations

Bedload transport equations are usually developed based on hydraulic principles and attempts to relate the level of bedload transport to several parameters such as water discharge, shear stress or stream power (Martin, 2003; Yang, 1972).

One of the main problems in measuring bed material transport is that, under natural conditions, bedload discharge is not a steady process and variations up to more than 50 percent may be expected (Dietrich and Gallinati, 1991). Because of difficulties in field measurements of bedload discharge, a large number of transport formulae have been developed for a wide range of sediment sizes and hydraulic conditions (Bagnold, 1980; Schoklitsch, 1934). Because of the relationship between the reliability and representativeness of the data utilized in defining reference values, constants, and other relevant coefficients and the performance of a particular equation, most sediment transport equations do not represent a fundamental or

complete correlation. Therefore it is really difficult, if not possible, to recommend a global equation for engineers to use in the field under all conditions (Camenen and Larson, 2005; Khorram and Ergil, 2010; Wu et al., 2000).

Numerous bed load transport equations have been formulated under limited laboratory or field conditions that are available in the literature (Habersack and Laronne, 2002). Table 2.1 to Table 2.7 are summary of bedload equations based on derivation approach with their name and years and cited references.

Table 2.1: Bedload transport equations, Deterministic Shear stress method

No	Name	Equation	Range of applicability	Cited references
1	Du Boys (1879)	$q_b = \tau_0 \left(\frac{0.173}{d_{50}^{3/4}} \right) (\tau_0 - 0.0125 - 0.019d_{50})$	$0.125 \leq d_{50} \leq 4.0$ (mm) $S_f > 0.00005$	(Yang, 1996)
2	Kalinske (1947)	$\frac{q_b}{u_* \gamma_s d_{50}} = f \left(\frac{\tau_{cr}}{\tau_0} \right)$	$0.088 \leq d_{35} \leq 45.3$ (mm) $S_f > 0.00005$	(Yang, 1996)
3	Grand and Albertson (1961)	$\frac{q_b}{u_* \gamma_s d_{50}} = f(\tau_0 - \tau_{cr})$	$0.088 \leq d_{50} \leq 45.3$ (mm)	(Yang, 1996)
4	Sato, Kikkawa and Ashida (1958)	$q_b \sqrt{G_s g} d_{50}^3 = \frac{u_*^3}{G_s g} F \left(\frac{u_*^2}{u_{*c}^2} \right) f(n)$ $F \left(\frac{u_*^2}{u_{*c}^2} \right) = \frac{1}{1 + 8 \left(\frac{u_{*c}^2}{u_*^2} \right)^4}$ $n \geq 0.025 : f(n) = 0.623$ $n < 0.025 : f(n) = 0.623(40n)^{-3.5}$	$20 \leq Re \leq 1000$ $0.088 \leq d_{50} \leq 5.66$ (mm)	(Garde and Raju, 2000)
5	Shields (1936)	$q_b = \frac{10q_s f(\tau_0 - \tau_{cr})}{(G_s - 1)\gamma d_{50}}$	$1.56 \leq d_{50} \leq 2.47$ (mm) $1.06 < G_s < 4.20$	(Yang, 1996)
6	Ribberink (1998)	$\varphi_b = 11(\theta - \theta_{cr})^{1.65}$	$0.088 \leq d_{50} \leq 2.83$ (mm)	(Ribberink, 1998)
7	Wilson (1996)	$\varphi_b = 12(\theta - \theta_{cr})^{3/2}$	$0.088 \leq d_{50} \leq 2.83$ (mm)	(Wilson, 1966)

Table 2.1: Continue

No	Name	Equation	Range of applicability	Cited references
8	Wong and Parker (2006)	$\varphi_b = \begin{cases} 4.93(\theta - 0.047)^{1.6} \\ 3.97(\theta - 0.0495)^{3/2} \end{cases}$	$0.088 \leq d_{50} \leq 4(\text{mm})$	(Wong and Parker, 2006)
9	Graf and Suszka (1987)	$\left\{ \begin{array}{l} \varphi_b = 12\theta^{1.5} \left(1 - \frac{0.045}{\theta}\right)^{2.5} \quad \theta < 0.068 \\ 10.5\theta^{2.5} \quad \theta \geq 0.068 \end{array} \right\}$	$0.088 \leq d_{50} \leq 4(\text{mm})$	(Graf, 1998)
10	Wiberg and Smith (1989)	$\varphi_b = \alpha_s (\theta - \theta_{cr})^{3/2}$ $\alpha_s = 9.64(\theta^{0.166})$	$0.088 \leq d_{35} \leq 5.66(\text{mm})$	(Wiberg and Smith, 1989)
11	Paintal (1971)	$16.56 \times 10^{18} \theta^{16}$	$1 \leq d_{50} \leq 25(\text{mm})$ $0.007 < \theta < 0.06$	(Paintal, 1971)
12	Low (1989)	$q_b = \frac{6.42}{(G_s - 1)^{0.5}} (\theta - \theta_{cr}) d_{50} v_{av} S_f^{0.5}$	$0.088 \leq d_{50} \leq 5.66(\text{mm})$ $\theta_{cr} = 0.06$	(Low, 1989)
13	Fernandez-Luque and Van Beek (1976)	$\varphi_b = 5.7(\theta - \theta_{cr})^{3/2}$	$0.9 \leq d_{50} \leq 3.3(\text{mm})$ $0.05 < \theta_{cr} < 0.058$	(Fernandez Luque and Van Beek, 1976)

Table 2.2: Bedload transport equations, Deterministic Stream power method

No	Name	Equation	Range of applicability	Cited references
1	Chang, Simons and Richardson (1967)	$q_b = K_t v_{av} (\tau_0 - \tau_{cr})$	$0.1 \leq K_t \leq 4(\text{mm})$ $0.19 \leq d_{50} \leq 0.93(\text{mm})$ $0.001 \leq S_f \leq 0.0005$	(Yang, 1996)
2	Dou (1964)	$q_b = 0.01 \left(\frac{\rho_s}{\rho_s - \rho} \right) \tau_0 (v_{av} - v_{cr}) \left(\frac{v_{av}}{g G_s} \right)$	$0.088 \leq d_{50} \leq 45.3(\text{mm})$	(Wu, 2007)
3	Bagnold (1966)	$q_b \times \left(\frac{\gamma_s - \gamma}{\gamma} \right) \tan \alpha = \tau_0 v_{av} e_b$	$0.088 \leq d_{50} \leq 1.41(\text{mm})$	(Bagnold, 1977)

Table 2.3: Bedload transport equations, Deterministic Energy slope method

No	Name	Equation	Range of applicability	Cited references
1	Meyer - Peter (1934)	$q_b = (250q^{2/3} s_f - 42.5d_{50})^{3/2}$	$3 \leq d_{50} \leq 29(\text{mm})$ $G_s = 2.65$ $R_h < 20$	(Yang, 1996)
2	Meyer - Peter and Muller (1948)	$\varphi_b = \begin{cases} 8(\theta - \theta_{cr})^{3/2} & \theta \geq \theta_{cr} \\ 0 & \theta < \theta_{cr} \end{cases}$	$0.4 \leq d_{50} \leq 30(\text{mm})$ $0.25 \leq G_s \leq 3.2$ $1 \leq R_h \leq 120(\text{cm})$ $0.0004 \leq S_f \leq 0.02$	(van Rijn, 1993)
3	Smart and Jaeggi (1983)	$\varphi_b = 4 \left(\frac{d_{90}}{d_{30}} \right) s_f^{0.06} \left(\frac{v_{av}}{u_*} \right) \theta^{0.5} (\theta - \theta_{cr})$	$0.088 \leq d_{50} \leq 2.83(\text{mm})$ $0.03 \leq S_f \leq 0.2$	(Smart and Jaeggi, 1983)
4	Pica (1972)	$q_b = 10.217 d_{50}^{-0.594} s_f^{1.681} q^{0.237}$	$0.088 \leq d_{50} \leq 45.3(\text{mm})$	(Pica, 1972)

Table 2.4: Bedload transport equations, Deterministic Regression method

No	Name	Equation	Range of applicability	Cited references
1	Abrahams and Gao (2006)	$\varphi_b = \theta^{1.5} \left(1 - \frac{\theta_{cr}}{\theta}\right)^{3.4} \left(\frac{v_{av}}{u_*}\right)$	$0.088 \leq d_{50} \leq 5.66(\text{mm})$	(Abrahams and Gao, 2006)
2	Nielsen (1992)	$\varphi_b = 12\theta^{1/2} (\theta - \theta_{cr})$	$0.69 \leq d_{50} \leq 28.7(\text{mm})$ $1.25 \leq G_s \leq 4.22$ $0.001 \leq S_f \leq 0.01$	(Nielsen, 1992)
3	Brown (1950)	$\varphi_b = \begin{cases} 2.15e^{-0.391\theta} & \theta < 0.068 \\ 40\theta^3 & 0.18 \leq \theta \leq 0.52 \\ 15\theta^{1.5} & \theta > 0.52 \end{cases}$	$0.088 \leq d_{50} \leq 45.3(\text{mm})$	(Julien, 2002)
4	Rottner (1959)	$q_b = \gamma_s R_h v_{av} \times \left[\begin{array}{l} \left[0.667 \left(\frac{d_{50}}{R_h} \right)^{2/3} + 0.14 \right]^3 \\ -0.778 \left(\frac{d_{50}}{R_h} \right)^{2/3} \end{array} \right]$	$0.088 \leq d_{50} \leq 45.3(\text{mm})$	(Yang, 1996)
5	England and Fredsoe (1976)	$\varphi_b = 18.74(\theta - \theta_{cr}) \left[\theta^{1/2} - 0.7(\theta_{cr})^{1/2} \right]$	$0.3 \leq d_{50} \leq 7(\text{mm})$ $\theta_{cr} = 0.05$	(Engelund and Fredsoe, 1982)

Table 2.4: Continue

No	Name	Equation	Range of applicability	Cited references
6	van Rijn (1984,1987,1993)	$\varphi_b = \frac{0.053}{D_*^{0.3}} \theta^{1.5} \left(\frac{\theta_{cr}}{\theta} - 1 \right)^{2.1}$	$0.2 \leq d_{50} \leq 2$ (mm) $Fr < 0.9$ $0.31 < v_{av} < 1.29$ m/s $0.001 \leq S_f \leq 0.01$ $0.1 \leq R_h \leq 1$ (m)	(van Rijn, 1993)
7	England and Hansen (1967)	$\varphi_b = 0.05 \left(\frac{v_{av}}{u_*} \right)^2 \theta^{5/2}$	$0.088 \leq d_{50} \leq 45.3$ (mm)	(Engelund and Hansen, 1967)
8	Fredsoe and Deigaard (1992)	$q_b = \frac{30}{\pi} (\theta - \theta_{cr}) (\theta^{1/2} - (\theta_{cr})^{1/2})$	$0.088 \leq d_{50} \leq 45.3$ (mm)	(Fredsoe and Deigaard, 1992)
9	Ashida and Michiue (1972)	$q_b = 17(\theta - \theta_{cr}) (\theta^{1/2} - (\theta_{cr})^{1/2})$	$0.088 \leq d_{50} \leq 45.3$ (mm) $\theta_{cr} = 0.05$	(Ashida, 1972)
10	Julien (2002)	$\varphi_b = \frac{18\sqrt{g} (d_{50})^{3/2} \theta^2}{\sqrt{g(G_s - 1)d_{50}^3}}$	$0.088 \leq d_{50} \leq 2.83$ (mm) $S_f > 0.0001$ $0.1 < \theta < 1.0$	(Julien, 2002)
11	Lefort Sogreah (1991)	$\frac{Q_s}{Q} = 4.45 \left(\frac{d_{90}}{d_{30}} \right)^{0.2} \left(\frac{\rho}{\rho_s - \rho} \right) S_f^{1.5} \left[1 - \left(\frac{Q_{tc}}{Q} \right)^{0.375} \right]$ $Q_{tc} = 0.295 S_f^{-13/6} (1 - 1.2 S_f)^{8/3} \sqrt{g d_{50}^5}$	$0.088 \leq d_{50} \leq 1.41$ (mm)	(Lefort, 1991)
12	Madsen (1991)	$\varphi_b = (\theta - \theta_{cr}) (\theta^{0.5} - 0.7 \theta_{cr}^{0.5})$	$0.088 \leq d_{50} \leq 5.66$ (mm)	(Madsen, 1991)
13	Smart (1983)	$q_b = 4\gamma \left[\sqrt{\left(\frac{\gamma_s - \gamma}{\gamma} \right) g d_{50}^3} \right] \times$ $\left[\left(\frac{d_{50}}{d_{90}} \right)^{0.2} S_f^{0.6} \frac{v_{av}}{u_*} \sqrt{\theta} (\theta - \theta_{cr}) \right]$	$d_{50} < 29$ (mm) $S_f < 0.2$	(van Rijn, 1993)
14	Nino and Garcia (1998)	$\varphi_b = \frac{12}{\mu_d} (\theta - \theta_{cr}) (\theta^{0.5} - 0.7 \theta_{cr}^{0.5})$	$0.088 \leq d_{50} \leq 5.66$ (mm) $\mu_d = 0.23$	(Nino and Garcia, 1998)

Table 2.4: Continue

No	Name	Equation	Range of applicability	Cited references
15	Rickenman (1990)	$\varphi_b = \frac{3.1}{(G_s - 1)^{0.5}} \left(\frac{d_{90}}{d_{30}} \right)^{0.2} \theta^{0.5} (\theta - \theta_{cr}) Fr^{1.1}$	0.088 ≤ d ₅₀ ≤ 5.66 (mm) 0.03 ≤ S _f ≤ 0.2 θ _{cr} = 0.05	(Rickenman, 1991)
16	Chang (2002)	$\varphi_b = 13\theta^{1.5} \exp\left(\frac{0.05}{\theta^{1.5}}\right)$	0.088 ≤ d ₅₀ ≤ 5.66 (mm)	(Cheng, 2002)
17	Camenen and Larson (2005)	$\varphi_b = 12\theta^{0.5} \exp\left(-4.5 \frac{\theta_{cr}}{\theta}\right)$	0.088 ≤ d ₅₀ ≤ 5.66 (mm)	(Camenen and Larson, 2005)
18	Bhattacharya, Price and Solomatine (2007)	$\varphi_b = \begin{cases} \frac{0.072078 T_*^{0.888}}{D_*^{0.353}} & T_* > 0.04 \\ \frac{0.000182 T_*^{0.13}}{D_*^{0.673}} & T_* \leq 0.04 \text{ and } D_* \leq 181.3 \\ \frac{0.0000124 T_*^{0.13}}{D_*^{0.673}} & T_* \leq 0.04 \text{ and } D_* > 181.3 \end{cases}$	0.088 ≤ d ₅₀ ≤ 5.66 (mm)	(Bhattacharya et al., 2007)

Table 2.5: Bedload transport equations, Deterministic Discharge and velocity method

No	Name	Equation	Range of applicability	Cited references
1	Casey (1935)	$q_b = 0.367 S_f^{9/8} (q - q_{cr})$ $q_{cr} = 6.5 \times 10^{-6} \left(\frac{d_{50}^{1.8}}{S_f^{0.5}} \right)$	0.0625 ≤ d ₅₀ ≤ 2 (mm)	(Casey, 1935)
2	Skoklitsch (1934)	$q_b = \frac{2.5}{\left(\frac{\rho_s}{\rho}\right)} S_f^{3/2} (q - q_{cr})$ $q_{cr} = 0.26 (G_s - 1)^{5/3} \times 10^{-6} \left(\frac{d_{50}^{1.5}}{S_f^{7/6}} \right) S_f > 0.003$	0.305 ≤ d ₅₀ ≤ 7.02 (mm) 0.24 < v _{av} ≤ 0.0876	(Yang, 1996)
3	Barekyan (1962)	$q_b = 0.187 q S_f \left(\frac{\gamma_s}{\gamma_s - \gamma} \right) \left(\frac{v_{av} - v_{cr}}{v_{cr}} \right)$	0.088 ≤ d ₅₀ ≤ 45.3 (mm)	(Barekyan, 1962)

Table 2.6: Bedload transport equations, Deterministic Equal mobility method

No	Name	Equation	Range of applicability	Cited references
1	Pitlick et al., (1990a,b)	$q_b = \frac{w^* u_*^3 \rho_s}{(G_s - 1)g}, \phi_{50} = \frac{\theta}{\theta_{cr}},$ $\theta = \frac{u_*^2}{(G_s - 1)gd_{50sub}}$ $W^* = \left\{ \begin{array}{l} \left\{ 11.9 \left(1 - \frac{0.853}{\phi_{50}} \right)^{4.5} \right\} \quad \phi_{50} > 1.59 \\ \left\{ 0.00218 \exp[14.2(\phi_{50} - 1)] - 9.28(\phi_{50} - 1)^2 \right\} \quad 1.0 \leq \phi_{50} \leq 1.59 \\ \left\{ 0.0025 \phi_{50}^{14.2} \right\} \quad \phi_{50} < 1.0 \end{array} \right\}$	$2.0 \leq d_{50} \leq 45.3$ (mm) $0.79 \leq v_{av} \leq 1.13$ (m/s) $2.9 \times 10^{-4} \leq S_f \leq 3.3 \times 10^{-3}$	(Pitlick et al., 2009)
2	Parker and Klingeman and Mclem (1982)	$q_b = \frac{w^* u_*^3 \rho_s}{(G_s - 1)g}, \phi_{50} = \frac{\theta}{\theta_{cr}},$ $\theta = \frac{u_*^2}{(G_s - 1)gd_{50sub}}$ $W^* = \left\{ \begin{array}{l} \left\{ 11.2 \left(1 - \frac{0.853}{\phi_{50}} \right)^{4.5} \right\} \quad \phi_{50} > 1.65 \\ \left\{ 0.0025 \exp[14.2(\phi_{50} - 1)] - (\phi_{50} - 1)^2 \right\} \quad 0.95 \leq \phi_{50} \leq 1.65 \\ \left\{ 0.0025 \phi_{50}^{14.2} \right\} \quad \phi_{50} < 0.95 \end{array} \right\}$	$2 \leq d_{50} \leq 45.3$ (mm) $S_f > 0.003$ $\theta_{cr} = 0.0876$	(Pitlick et al., 2009)
3	Parker and Klingeman (1982)	$q_b = \frac{w^* u_*^3 \rho_s}{u_*^3} = 11.2 \times \left[1 - \frac{0.0747}{\theta} \left(\frac{d_i}{d_{50}} \right)^{0.018} \right]^{4.5}$ $\phi_{50} = \frac{\theta}{\theta_{cr}}, \quad \theta = \frac{u_*^2}{(G_s - 1)gd_{50sub}}$	$2 \leq d_{50} \leq 45.3$ (mm) $S_f > 0.003$ $\theta_{cr} = 0.0876$	(Pitlick et al., 2009)
4	Wilcock (2001)	$q_b = \frac{w^* u_*^3 \rho_s}{(G_s - 1)g}$ $W_g^* = \left\{ \begin{array}{l} \left\{ 11.2 \left(1 - 0.846 \frac{\tau_{cr}}{\tau_0} \right)^{4.5} \right\} \quad \tau_0 > \tau_{cr} \\ \left\{ 0.0025 \left(\frac{\tau_0}{\tau_{cr}} \right) \right\} \quad \tau_0 \leq \tau_{cr} \end{array} \right\}$ $\theta = \frac{u_*^2}{(G_s - 1)gd_{50sub}}, \quad \phi_{50} = \frac{\theta}{\theta_{cr}}$	$2.0 \leq d_{50} \leq 45.3$ (mm)	(Pitlick et al., 2009)
5	Wilcock and Crowe (2003)	$q_b = \frac{w^* u_*^3 \rho_s}{(G_s - 1)g}, \quad \phi_{50} = \frac{\theta}{\theta_{cr}},$ $\theta = \frac{u_*^2}{(G_s - 1)gd_{50sub}}$ $W^* = \left\{ \begin{array}{l} \left\{ 14 \left(1 - \frac{0.853}{\phi_{50}^{0.5}} \right)^{4.5} \right\} \quad \phi_{50} \geq 1.35 \\ \left\{ 0.002 \phi^{7.5} \right\} \quad \phi_{50} < 1.35 \end{array} \right\}$	$2.0 \leq d_{50} \leq 45.3$ (mm)	(Pitlick et al., 2009)

Table 2.7: Bedload transport equations, Deterministic Probabilistic method

No	Name	Equation	Range of applicability	Cited references
1	Einstein (1942 and 1950)	$\varphi_b = \frac{q_b}{\gamma_s} \sqrt{\frac{\gamma}{\gamma_s - \gamma}} \sqrt{\frac{1}{gd_{50}^3}}$	$0.315 \leq d_{50} \leq 28.6$ (mm) $1.25 \leq G_s \leq 4.25$	(van Rijn, 1993)
2	Einstein-Brown (1950)	$\varphi_b = \begin{cases} \frac{k \exp(-391/\theta)}{0.465} & \theta < 0.182 \\ 40k\theta^3 & \theta \geq 0.182 \end{cases}$	$0.088 \leq d_{50} \leq 5.66$ (mm)	(Yang, 1996)
3	Gill (1972)	$\varphi_b = 40 \left(\frac{\tau_{cr}}{\tau_0} - 1 \right)^3$	$0.088 \leq d_{50} \leq 2.83$ (mm)	(Gill, 1972)
4	Parker (1979)	$\varphi_b = 11.20 \frac{(\theta - 0.03)^{4.5} \theta_{cr}}{\theta^3}$	$2.83 \leq d_{50} \leq 5.66$ (mm) $0.00035 \leq S_f \leq 0.0108$	(Pitlick et al., 2009)
5	Yalin (1963)	$\varphi_b = 0.635r\sqrt{\theta} \left[1 - \frac{1}{r\sigma} \ln(1+r\sigma) \right]$ $r = \frac{\theta}{\theta_{cr}} - 1, \sigma = 2.45 \frac{\sqrt{\theta_{cr}}}{(\rho_s/\rho)^{0.4}}$	$0.315 \leq d_{50} \leq 28.65$ (mm)	(van Rijn, 1993)

2.4.1 Performance of Bedload Transport Equations

Gomez and Church (1989) used 88 bedload transport observations from 4 natural gravel bed rivers and 45 bedload transport observation from 3 flumes to analyse some bedload transport equations. The authors conclude that there is no equation to be tested performed consistently well, due to limited data used and the complexity of transport occurrence. They found the best prediction of bedload transport under limited hydraulic information is achieved by using equations based on the power flow concept.

The performance of 13 sediment transport formula in terms of their ability to describe sediment transport was tested by Yang and Huang (2001) . They achieved that the sediment transportation formulae based on the level of energy dissipation or the concept of power flow, more accurately describe transported observed data. Also the rate formulae complexity does not always translate into increased model accuracy.

Prior to the extensive work of Yang and Huang (2001), Barry et al. (2004) performed simple regressions to complex multi-parameter formulation for 24 gravel bed rivers with 2104 bedload transport observation in Idaho to evaluate the fitness of eight different formulations of four bedload transport equations. The authors concluded that there was no reliable relationship between formulae performance and degree of calibration or complication. They found that transport data were best described by a simple power function of discharge. They proposed a new bedload transport equation and identify the channel and watershed characteristics effect on the proposed power function by controlling the exponent and coefficient.

The ability of the deterministic empirical equations of van Rijn (1984, 1993) and Meyer-Peter and Muller (1948) was assessed by Claude et al. (2012) for a large sand–gravel bed river to determine the unit and total bedload transport rates by comparing bedload discharges obtained from bedload measurements with predictions. The authors concluded that the tested equations were unable to predict the daily temporal variations of the total bedload transport at low and medium flow conditions. The formulas described the bedload hysteresis but underestimated its magnitude. For high flow conditions, the best agreement was observed for the total

bedload discharges computed by the van Rijn equation. The obtained results indicated that the empirical equations only able to predict the temporal variations of bedload transport if the flow velocities followed a similar trend.

The equations of Meyer-Peter and Mueller (1948), Einstein-Brown (1950), Schoklitsch (1950), Frijlink (1952), Yalin (1963), Bagnold (1980), Engelund and Hansen (1967), Bijker (1971), Ackers and White (1973), Parker et al. (1982), van Rijn (1984, 1987) and Cheng were evaluated with measured bedload by a Helley-Smith sampler in the Node River, a gravel bed river in the northeast part of Iran (Haddadchi et al., 2012). The results indicated that the statistic equation such as van Rijn- Stochastic, Einstein and Bijker were not able to predict bed load in that gravel bed river. Van Rijn, Frijlink and Myer-Peter and Mueller equations based on shear stress achieved good results while some of them like Yalin and Cheng's gave very poor results. Equations based on the energy concept including Bagnold and Engelund and Hansen equations tended to overestimate the real state in that river. Generally the equations presented by van Rijn, Meyer-Peter and Mueller, and Ackers and White might tolerably predict bedload transport in the range of field data of Node River.

2.5 Regression Analysis

2.5.1 Linear Regression

Regression is a highly useful statistical method to determine a quantitative relation between one or more independent variables and a dependent variable. Throughout engineering, regression may be applied to correlating data in a wide variety of problems ranging from simple to complex physical and industrial systems. If nothing is known a function may be assumed and fitted to experimental data on the

system. In other cases where the result of linear regression is unacceptable other method such as nonlinear regression may give better results.

Simple linear regression is a relationship between a response variable Y and a single explanatory variable X . In the simplest case the proposed functional relation is:

$$Y = \beta_0 + \beta_1 X + \varepsilon \quad (2-1)$$

In this model ε is a random error (or residual) which is the amount of variation in Y not accounted by linear regression. The parameters β_0 and β_1 , called the regression coefficients, are unknown and to be estimated. It will be assumed that the error ε is independent and have a normal distribution with mean zero and variance σ^2 , regardless of what fixed value of X is being considered. Then the value of β_0 and β_1 can be estimated by the method of the last squares (Bethea et al., 1995).

2.5.2 Multiple Linear Regression

The multiple linear regression is similar to simple linear regression except that a number of independent variables, X_1, X_2, \dots, X_p , have relationship to a single dependent variable Y (Bethea et al., 1995). The general form of the multiple regression method is given by:

$$Y = \beta_0 + \beta_1 X_1 + \beta_2 X_2 + \dots + \beta_p X_p + \varepsilon \quad (2-2)$$

where the ε is random error (or residual). The general form of multiple linear regressions is shown below using logarithmic transformation

$$\ln Y = \ln \beta_0 + \beta_1 \ln(X_1) + \beta_2 \ln(X_2) + \dots + \beta_p \ln(X_p) + \varepsilon_1 \quad (2-3)$$

or

$$Y = \beta_0(X_1)^{\beta_1}(X_2)^{\beta_2} \dots (X_p)^{\beta_p} \quad (2-4)$$

The regression coefficients (β_i) are same to simple regression and can be obtained from last square technique.

2.5.3 Least- Square Method

The least-square method is probably the most popular technique in statistics. The method has been adopted to find the best-fit line or curve from a given set of data. In the standard formulation, a set of N pairs of observations $\{Y_i, X_i\}$ is used to find a function relating the value of the dependent variable Y to the values of an independent variable X . Assume that the set of data points are $(x_1, y_1), (x_2, y_2), \dots, (x_p, y_p)$ where x is the independent variable and y is dependent variable. The fitting curve $f(x)$ has the deviation (error) of ε from each data point, i.e., $\varepsilon_1 = y_1 - f(x_1), \varepsilon_2 = y_2 - f(x_2), \dots, \varepsilon_p = y_p - f(x_p)$. According to the method of least squares, the best fitting curve has the property that:

$$SS_E = \varepsilon_1^2 + \varepsilon_2^2 + \dots + \varepsilon_p^2 = \sum_{i=1}^p \varepsilon_i^2 = \sum_{i=1}^p [y_i - f(x)]^2 = \text{minimum} \quad (2-5)$$

If suppose the $f(x)$ is a simple linear function then

$$SS_E = \sum_{i=1}^p [y_i - \beta_0 + \beta_1 X_i]^2 = \text{minimum} \quad (2-6)$$

To determine the minimum sum of square due to error (SS_E), the partial derivative of SS_E which respect to each constant (β_0, β_1) is set equal to zero to yield:

$$\frac{\partial(SS_E)}{\partial\beta_0} = \frac{\partial}{\partial\beta_0} \left[\sum_{i=1}^p (y_i - \beta_0 + \beta_1 X_i)^2 \right] = 0 \quad (2-7)$$

$$\frac{\partial(SS_E)}{\partial\beta_1} = \frac{\partial}{\partial\beta_1} \left[\sum_{i=1}^p (y_i - \beta_0 + \beta_1 X_i)^2 \right] = 0 \quad (2-8)$$

The solutions of these equations are

$$\beta_0 = \bar{Y} - \beta_1 \bar{X} \quad (2-9)$$

$$\beta_1 = \frac{\sum_i (X_i - \bar{X})(Y_i - \bar{Y})}{\sum_i (X_i - \bar{X})^2} \quad (2-10)$$

This solution for estimation of β_0 , β_1 is called least-square solution. For multi linear regression this method can be used to determine the regression coefficients of β_i .

2.5.4 Polynomial Regression

In the case of polynomial or curvilinear regression, as given by the model:

$$Y = \beta_0 + \beta_1 X + \beta_2 X^2 + \dots + \beta_p X^p + \varepsilon \quad (2-11)$$

there is only one independent variable (X). Therefore the power of X can be considered as $W_1=X$, $W_2=X^2, \dots$, $W_p=X^p$ and the model is reduced to multiple regression as given by Equation (2.2).

2.5.5 Nonlinear Regression

Nonlinear regression is a method of finding a nonlinear model of the relationship between the dependent variable and a set of independent variables. The nonlinear regression is utilized when no linearizing transformation can be found (Bethea et al., 1995). This procedure estimates the parameter value that minimizes